Structural Motifs of the Dimeric Lewis Glycolipids as Determined by NMR Spectroscopy and Molecular Dynamics Simulations

Armin Geyer,* Gerd Hummel, Thomas Eisele, Stefan Reinhardt and Richard R. Schmidt*

Abstract: Several monomeric and dimeric Lewis glycolipids have been investigated by NMR spectroscopy, and structural aspects were modelled by computer. From the pseudo-C_2-symmetric tetrasaccharide unit that forms the recognition domain of the Lewis Y and Lewis b antigens, a totally C_2-symmetric tetrasaccharide was designed that contains the structural element common to all Lewis antigens. Finally, a model for the presentation of dimeric Lewis antigens at membrane surfaces was derived. The overall shapes of the dimeric Lewis oligosaccharides are defined by the connectivity of the sugar residues within rigid tri- and tetrasaccharide building blocks.

Keywords
computer simulations · conformations · Lewis glycolipids · molecular dynamics · thioglycosides

Introduction

Lewis glycoconjugates are expressed in various forms at the surface of eucaryotic cells and have attracted interest in recent years as tumour-associated antigens.[1] They also act as binding epitopes in transient cell recognition by initiating the rolling of leucocytes over the endothelial cell wall,[2] or by mediating the first steps of bacterial or viral infections.[3]

Homogeneous glycoconjugates are obtained by chemical synthesis; partial[4] and total syntheses[5] have been reported. Lewis oligosaccharides have been investigated with great computational effort since the pioneering work of Lemieux,[6] and although the spatial structures seem to be well-defined, the extent of flexibility remains unclear.[7, 8] NMR spectroscopic data are very sensitive towards conformational averaging and allow the identification of flexible and rigid domains in biopolymers. The extent of averaging of NMR data is difficult to quantify for oligosaccharides, for which often only few interglycosidic NOE data are available.[9, 10]

With several monomeric and dimeric Lewis oligosaccharides at hand,[11] we could control the reproducibility and reliability of NOE-derived distance restraints. We looked for common structural features within the Lewis antigens and tested our conclusions by comparing the natural structures with two synthetic mimetics. One tetrasaccharide of very different connectivity, namely Fucα(1 → 2)-Galβ,β-trehalose, possessing the same structural characteristics as the natural oligosaccharides exhibits a nearly identical NOE pattern and thus the same conformation. A second analogue, where minimal structural modifications—namely exchange of anomeric sulfur for oxygen—destroy the stabilizing interactions typical of the Lewis antigens, demonstrates a conformational behaviour which is not comparable to that of the natural Lewis oligosaccharides.

[*] Dr. A. Geyer, Dipl. Chem. G. Hummel, Dipl. Chem. T. Eisele, Dipl. Chem. S. Reinhardt, Prof. Dr. R. R. Schmidt
Fakultät Chemie, Universität Konstanz
Postfach 5560 M 725, D-78434 Konstanz (Germany)
Fax: Int. code +(7531)88-3135

Results and Discussion

Data acquisition and interpretation: NOESY spectra[12] of tetra- and pentasaccharides usually exhibit weak cross-signal intensities owing to the intermediate molecular tumbling rates with correlation times of the order of the inverse of the spectrometer frequency. The mobility of small molecules can be slowed down at the surface of [D_{25}]sodium dodecylsulfate (SDS) micelles in D_2O; the consequence is NOESY spectra of higher intensity, as they are observed only for larger molecules. Originally, deuterated micelles were employed to study the conformational behaviour of peptides in a membrane-mimetic environment,[13] but this method also works very well for a micellar solution of Lewis glycosphingolipids (Scheme 1) where only the fatty acid chains insert into the micelles and the oligosaccharide domains retain most of their conformational degrees of freedom. ^{1}H NMR signals are very sensitive towards environmental influences, and line broadening (Fig. 1) confirms the insertion of the glycosphingolipids into the micelle surfaces. The relative chemical shift differences remain unaffected, indicating that no conformational changes are induced in the oligosaccharide moieties by the change between the two different solvent environments.

Though a micellar environment favours spin diffusion, NOESY spectra with sufficiently short mixing times can be interpreted according to the two-spin approximation.[14] It was shown that this is applicable to glycolipids too;[15, 16] NOESY spectra for the monomeric Lewis antigens were acquired under these conditions (Fig. 2).

The dimeric Lewis antigens, which are assembled from nine sugar residues (Scheme 1) and thus have longer correlation times than the monomeric antigens, exhibit intense negative

 0947-6539/96/0208-0980 $ 15.00+.25/0

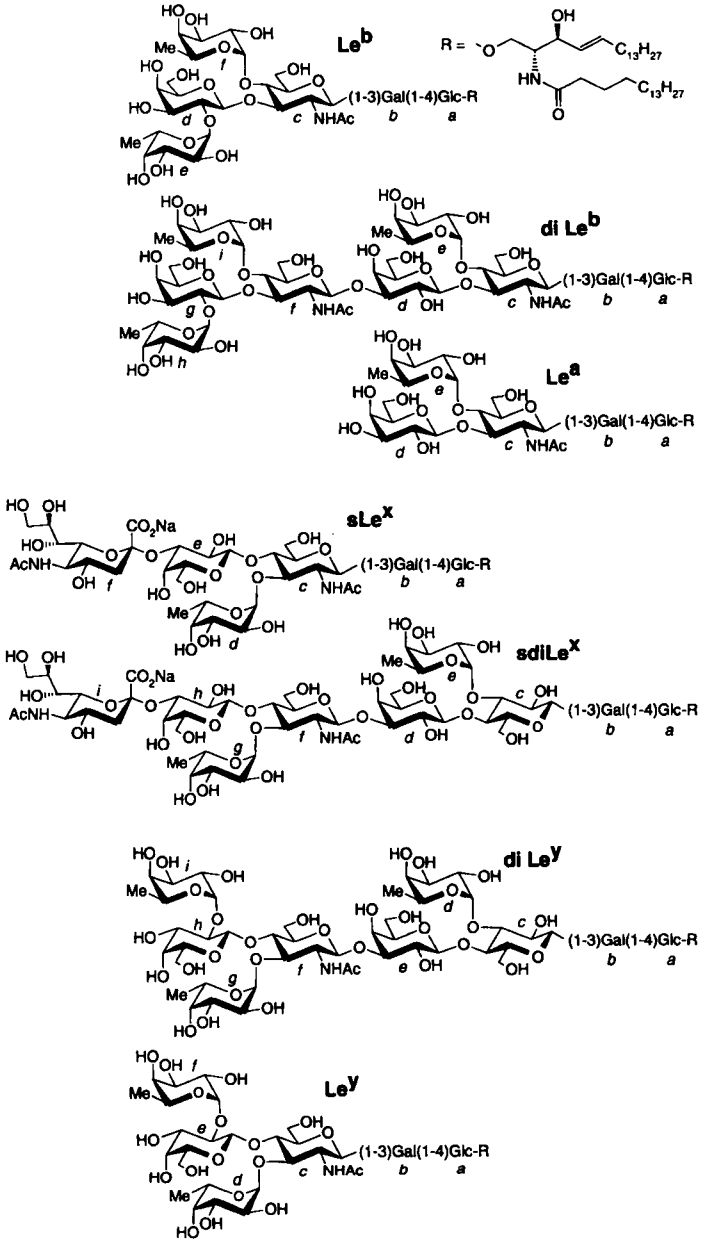

Scheme 1.

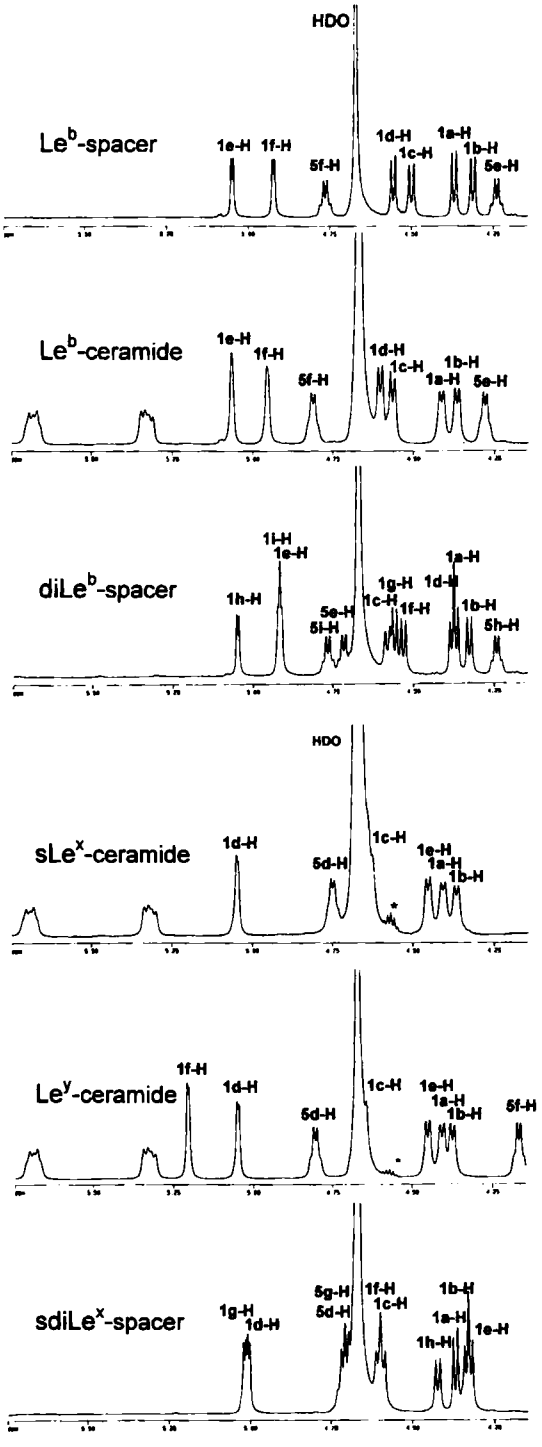

Fig. 1. Anomeric regions of the ^{1}H NMR spectra (300 K, 600 MHz) of several monomeric and dimeric Lewis antigens under different solvent conditions. Le^b with a ceramide aglycon in a micellar solution of fully deuterated SDS in D_2O differs from Le^b with a short alkyl aglycon in pure D_2O by a lowfield shift of $\Delta\delta$ = 0.02–0.04 ppm for all signals. The relative positioning of the anomeric protons remains unaffected and all resonance signals exhibit similar line broadening. The same effects are visible in the NMR spectra of sLe^x and Le^y. The two signals at lowest field are the olefinic protons of ceramide. 98.4% [D_{25}]SDS resonance signals are marked by asterisks. Repetitive units in the dimeric Lewis antigens are not fully resolved in SDS micelles; spectral quality is better in pure D_2O.

NOEs in pure D_2O (R = $C_6H_{12}N_3$). The reduced line broadening in pure D_2O allowed the assignment of several NOEs which are not resolved for the dimeric Lewis antigens (R = ceramide) in SDS micelles. Thus, for monomeric Lewis oligosaccharides it was advantageous to acquire NOESY spectra of the natural glycosphingolipids in the membrane-mimetic environment of SDS micelles ($\Rightarrow$ intense NOEs), while for dimeric Lewis antigens an investigation of the oligosaccharide moiety in pure D_2O was the better choice ($\Rightarrow$ improved signal resolution).

Interglycosidic NOEs for Le^a, Le^b and diLe^b are listed in Table 1. The oligosaccharides contain the branched trisaccharide unit Galβ(1 $\rightarrow$ 3)[Fucα(1 $\rightarrow$ 4)]GlcNAcβ with varying substitution patterns (Scheme 1). Even the long-range NOEs between sugars not directly connected (bold in Table 1) are similar for the three oligosaccharides; deviations are within the 10% range of experimental error. Long-range NOEs are very sensitive towards conformational changes, since they are influenced by several variable torsion angles.

NOE-derived proton–proton distances from Table 1 served as the restraints in individual molecular dynamics (MD) simulations of Le^a, Le^b and diLe^b. Ten structures from a 100 ps MD simulation of each oligosaccharide were averaged and energy-

0947-6539/96/0208-0982 $ 15.00+.25/0 Chem. Eur. J. 1996, 2, No. 8

Table 1. The columns labelled "r" contain the experimentally derived proton–proton distance restraints. The columns labelled "MD" contain the distances in an averaged and energy-minimized molecular dynamics simulation (all distances in pm). Distances of comparable building blocks are listed in the same row; sugars are numbered along the branching points. Short distances between monosaccharides not directly connected are in boldface. Diastereotopic assignment of terminal methylene groups was not possible and a long, less restraining distance of 320 pm was used in the MD simulations (experimental distances to methylene groups are listed in the footnotes). n.d. = Not determined, s. = signal overlap.

Le^a [a]	r	MD	$diLe^b$ [b]	r	MD
1d-H–3c-H	260	245	1d-H–3c-H	240	242
1e-H–4c-H	270	236	1e-H–4c-H	s.	250
1e-H–5c-H	330	370	1e-H–5c-H	n.d.	371
5e-H–3c-H	330	356	5e-H–3c-H	n.d.	366
5e-H–2d-H	**280**	**265**	**5e-H–2d-H**	**240**	**265**
1e-H–6c-H^{proR}	320	261	1e-H–6c-H^{proR}	320	255
1e-H–6c-H^{proS}	320	227	1e-H–6c-H^{proS}	320	240
Le^b [c]	r	MD	1f-H–3d-H	220	213
			1f-H–4d-H	360	314
1d-H–3c-H	260	253	1g-H–3f-H	250	258
5e-H–2d-H	370	346	5h-H–2g-H	n.d.	350
1e-H–2d-H	250	230	1h-H–2g-H	240	228
5e-H–2c-H	**260**	**253**	**5h-H–2f-H**	**240**	**244**
5f-H–3c-H	320	358	5i-H–3f-H	n.d.	365
5f-H–2d-H	**250**	**243**	**5i-H–2g-H**	**250**	**248**
1f-H–4c-H	260	247	1i-H–4g-H	s.	229
1f-H–5c-H	340	367	1i-H–5f-H	n.d.	382
1f-H–6c-H^{proR}	320	379	1i-H–6f-H^{proR}	320	376
1f-H–6c-H^{proS}	320	243	1i-H–6f-H^{proS}	320	238

[a] 1e-H–6c-$H^{low\ field}$ = 260 pm, 1e-H–6c-$H^{high\ field}$ = 230. [b] 1e-H and 1i-H are not resolved: 1e-H–6c-$H^{low\ field}$, 1i-H–6f-$H^{low\ field}$ = 260 pm, 1e-H–6c-$H^{high\ field}$, 1i-H–6f-$H^{high\ field}$ = 240 pm. [c] 1f-H–6c-$H^{low\ field}$ = 250 pm, 1f-H–6c-$H^{high\ field}$ = 230.

minimized; proton–proton distances are listed in Table 1. Deviations are observed for the terminal methylene groups, where experimental distances that are too short are not reproduced in the MD simulation (footnotes in Table 1). The r^{-6} dependence of the NOE leads to an excessive contribution from strong NOE contacts in the rotational motion of the methylene groups. Such too-short distances are the result of averaging between two or more states of similar energy content. The experimental NOEs within the branched carbohydrate moieties correspond well to a low-energy conformer for each carbohydrate in Table 1. Experimentally derived distances are best reproduced for Le^b, for which the highest ratio of restraints per residue was available.

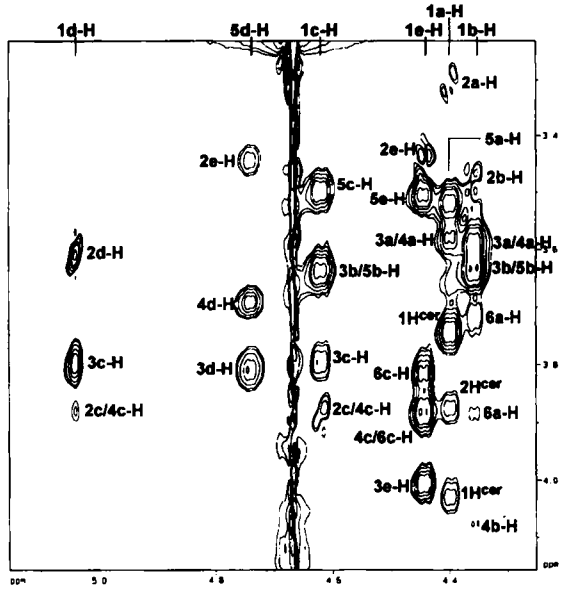

Fig. 2. Expansion of the NOESY spectrum (300 K, 600 MHz) of sLe^x with a ceramide aglycon in SDS micelles. Sugars are numbered according to Scheme 1; ceramide protons are denoted by "cer". The NOEs are evaluated in Table 2.

Even for Le^a, where few experimental restraints were available, the deviation between experimental data and the low-energy conformer is only 11%. An averaged and energy-minimized representation of $diLe^b$ is shown in Figure 3. Glycosidic angles for sugar f of $diLe^b$ (Scheme 1) are 41° (ϕ) and −40° (ψ); other relevant torsion angles are listed in Table 3. The branched building blocks are connected to lactose by a GlcNAcβ(1 → 3)Gal bond. In the case of $diLe^b$ this linkage is defined by the NOEs 1c-H–3b-H (230 pm) and 1c-H–4b-H (350 pm) (similar distances were determined for the other glycolipids). The glycosidic angles generally vary about the equilibrium values of $\phi = 50°$ (ϕ = H$^{1'}$-C$^{1'}$-O^3-C^3) and $\psi = -40°$ (ψ = C$^{1'}$-O^3-C^3-H^3). The Galβ(1 → 4)Glc bond of lactose[17] is defined by the NOEs 1b-H–4a-H (220 pm) and 1b-H–6a-H^{proR} (330 pm) and 1b-H–6a-H^{proS} (290 pm); angles fluctuate around $\phi = 50°$ and $\psi = 0°$.

The glycosidic torsion angles within the branched tri- and tetrasaccharide building blocks of Le^a, Le^b and $diLe^b$ in Table 3

Table 2. Columns with proton–proton distances are arranged to contain the terminal trisaccharide unit (c, d, e for sLe^x and Le^y; f, g, h for $sdiLe^x$ and $diLe^y$) in one row. Further details are given in Table 1.

sLe^x [a]	r	MD	$sdiLe^x$ [b]	r	MD	$diLe^y$ [c]	r	MD	Le^y [d]	r	MD
			1d-H–3c-H	260	255	1d-H–3c-H	275	261			
			6d-H–2e-H	**350**	**377**	**5d-H–2e-H**	**260**	**252**			
			1e-H–6c-H^{proR}	320	278	1e-H–6c-H^{proR}	320	285			
			1e-H–6c-H^{proS}	320	272	1e-H–6c-H^{proS}	320	294			
			1f-H–3e-H	230	221	1f-H–3e-H	230	217			
			1f-H–4e-H	350	334	1f-H–4e-H	n.d.	377			
1d-H–3c-H	260	255	1g-H–3f-H	260	255	1g-H–3f-H	280	267	1d-H–3c-H	260	289
5d-H–2e-H	**280**	**244**	**6g-H–2h-H**	**350**	**371**	**6g-H–2h-H**	**280**	**270**	**5d-H–2e-H**	**260**	**303**
1e-H–4c-H	s.	235	1h-H–4f-H	s.	226	1h-H–4f-H	250	226	1e-H–4c-H	240	219
1e-H–6c-H^{proR}	320	273	1h-H–6f-H^{proR}	320	276	1h-H–6f-H^{proR}	320	286	1e-H–6c-H^{proR}	320	281
1e-H–6c-H^{proS}	320	242	1h-H–6f-H^{proS}	320	265	1h-H–6f-H^{proS}	320	257	1e-H–6c-H^{proS}	320	270
						1i-H–2h-H	290	253	1f-H–2e-H	260	247
						5i-H–5f-H	**280**	**266**	**5f-H–5c-H**	**280**	**313**
						5i-H–6f-H^{proR}	320	438	5f-H–6c-H^{proR}	320	438
						5i-H–6f-H^{proS}	320	276	5f-H–6c-H^{proS}	320	269

[a] 6c-$H^{low\ field}$ and 4c-H overlap; 1d-H–6c-$H^{high\ field}$ = 240; 3f-H^{ax}–3e-H = 340 pm. [b] Only the terminal methyl groups are sufficiently resolved for d and g; therefore the 6d-H–2e-H and 6g-H–2h-H distances were determined. 6c/f-$H^{low\ field}$ and 4c/f-H overlap for the repetitive trisaccharide units; 1d/g-H–6c/f-$H^{high\ field}$ = 230; 3i-H^{ax}–3h-H = 340 pm. [c] 6c-$H^{low\ field}$ and 4c-H overlap; 1d-H–6c-$H^{high\ field}$ = 250; 6f-$H^{high\ field}$, 4i-H and 3f-H overlap; 1h-H–6f-$H^{low\ field}$ = 260 pm, 5i-H–6f-$H^{low\ field}$ = 230 pm. [d] 6c-$H^{high\ field}$, 4f-H and 3c-H overlap; 1e-H–6c-$H^{low\ field}$ = 250 pm, 5f-H–6c-$H^{low\ field}$ = 290 pm.

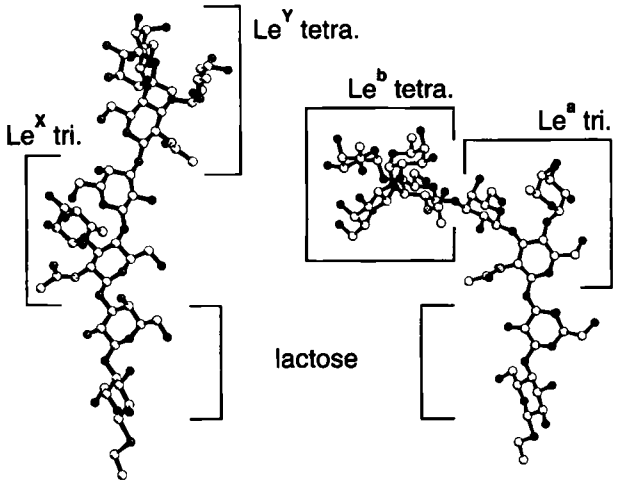

Fig. 3. Carbohydrate moieties of the Lewis antigens diLe^y (left) and diLe^b (right) averaged over 100 ps of MD simulation with experimental restraints and followed by energy minimization. The central Le^x trisaccharide moiety stabilizes the linear structure of diLe^y. The central Le^a moiety of diLe^b stabilizes the bent conformation of this glycolipid. The rigid tri- and tetrasaccharide units are connected by less restrained GlcNAc(1 → 3)Gal linkages.

Table 3. Glycosidic angles (°) of the Lewis oligosaccharides (ϕ = H$^{1'}$-C$^{1'}$-O^x-C^x, ψ = C$^{1'}$-O^x-C^x-H^x). Dimeric Lewis antigens are listed twice for their first (1) and second (2) repetitive unit (Scheme 1). Average values are denoted by "av".

	Fucα(1 → 4)GlcNAcβ		Galβ(1 → 3)GlcNAcβ		Fucα(1 → 2)Galβ	
	ϕ	ψ	ϕ	ψ	ϕ	ψ
Le^a	43	20	52	21	–	–
Le^b	39	23	54	24	49	22
diLe^b (1)	52	22	45	26	–	–
diLe^b (2)	44	16	54	29	37	21
av	45	20	51	25	43	22
	Fucα(1 → 3)GlcNAcβ		Galβ(1 → 4)GlcNAcβ		Fucα(1 → 2)Galβ	
	ϕ	ψ	ϕ	ψ	ϕ	ψ
sLe^x	52	29	55	7	–	–
sdiLe^x (1)	50	30	54	−1	–	–
sdiLe^x (2)	50	31	54	1	–	–
Le^y	59	38	58	0	42	31
diLe^y (1)	55	31	57	−6	–	–
diLe^y (2)	57	33	49	3	52	27
av	54	32	55	1	47	29

are retained throughout the Le$^{a/b}$ series (average torsion angles are listed under "av"). These angles were used for the representation of the Le^a tri- and Le^b tetrasaccharide units in Figure 4. The same procedure was applied to four representative oligosaccharides of the Le$^{x/y}$ series (Table 2). The branched trisaccharide unit Galβ(1 → 4)[Fucα(1 → 3)]GlcNAcβ recurs with different substitution patterns in the series (Scheme 1) and several NOEs are conserved (Table 2); these again served as distance restraints for four individual MD simulations. An averaged energy-minimized structure of diLe^y is shown in Figure 3. Torsion angles determined for sugar f of diLe^y are 54° (ϕ) and −25° (ψ); torsion angles for sugar f of sdiLe^x are 52° (ϕ) and −38° (ψ). NOEs within the lactose unit are similar to those observed for the Le$^{a/b}$ series. Glycosidic angles are listed in Table 3. The averaged torsion angles were taken for Le^x trisaccharide and the Le^y tetrasaccharide of Figure 4.

For the Neu5Acα(2 → 3)Gal linkage, only one strong transglycosidic NOE could be detected (Table 2); this does not permit the restriction of two glycosidic angles. Sialic acid rotated freely in the MD simulations of sLe^x and sdiLe^x; we could not determine one dominating energetic minimum. The Neu5Acα(2 → 3)-Gal linkage obviously populates more than one energetic minimum in solution.[18] Since sialic acid does not influence the conformational behaviour of the branched building blocks of sLe^x and sdiLe^x (Table 2), it is therefore neglected in the following analysis.

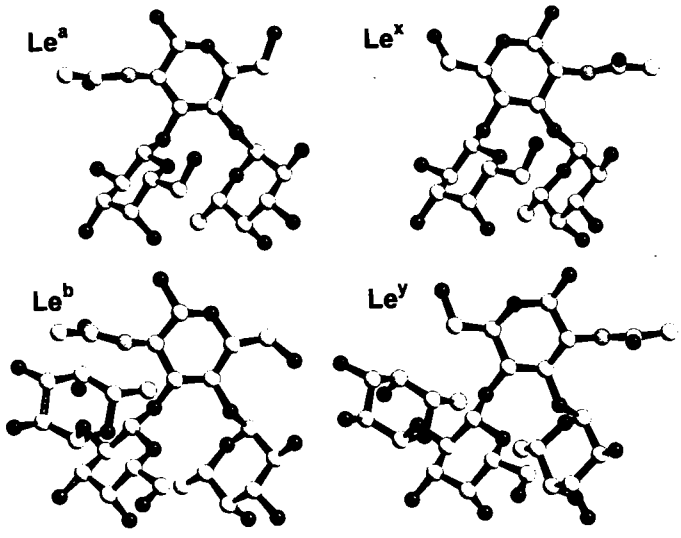

Fig. 4. Le^x and Le^a trisaccharides and Le^y and Le^b tetrasaccharides are the building blocks for oligomeric Lewis antigens. Averaged glycosidic angles from Table 3 were used for this representation. A 180° flip of *N*-acetylglucosamine around its pyranose ring plane transforms the Le$^{x/y}$ series into the Le$^{a/b}$ series. The relative orientation of fucose and galactose moieties remains unchanged.

The similarity between Le^x and Le^a trisaccharides has been pointed out in earlier studies.[6, 7, 8] The Le^x trisaccharide is transformed into the Le^a trisaccharide by turning *N*-acetylglucosamine 180° around its ring plane. The relative orientation of fucose and galactose remains unaffected (Fig. 4). This conformational similarity of the trisaccharide building blocks is strictly maintained throughout the naturally occuring gangliosides and sphingolipids in Scheme 1. The NOE between the fucose and galactose that are not directly connected in the branched trisaccharide units (bold in Tables 1 and 2) varies between 250 and 280 pm, well within the range of experimental error.[43]

Le^b, diLe^b, Le^y and diLe^y contain an additional fucose moiety which is connected α-glycosidically to the 2-O of galactose. The 5-H of this fucose shows an intense NOE (260 pm ± 10%) to 2-H of the preceeding *N*-acetylglucosamine in the Le^b series and to 5-H of *N*-acetylglucosamine in the Le^y series. A 180° flip of *N*-acetylglucosamine around its ring plane transforms the Le^b tetrasaccharide into the Le^y tetrasaccharide and moves 2-H to the position of 5-H (Fig. 4) but again has no influence on the NOE intensity.

Fast-equilibrating conformational states lead to averaged NOEs from which unwanted, so-called virtual conformations are derived; their analysis is only possible with additional experimental data.[19] Since conformational equilibria are very sensitive towards a changing chemical environment, minor structural modifications will strongly influence the NOE pattern. Invariable NOE intensities are observed within the branched tri- and tetrasaccharide building blocks of the Lewis oligosaccharides, where a changing connectivity and number of sugar substituents definitely would influence conformational averaging.[20] This preserved NOE pattern is strong evidence for conformational homogeneity within this series of oligosaccharides, and the structural similarity within the Le^x and Le^a trisaccharide units (Le^y and Le^b tetrasaccharide units) can be confirmed indepen-

0947-6539/96/0208-0984 $ 15.00+.25/0 Chem. Eur. J. 1996, 2, No. 8

dently from the model employed to derive proton–proton distance restraints from NOEs.

Steric hindrance, hydrophobic interactions, and the *exo*-anomeric effect contribute to the stability of the Lewis antigens.[8] Le^y and Le^b tetrasaccharides are exceedingly rigid carbohydrate structures, created to be presented as conformationally stable recognition domains at the cell surface. The stability of the tetrasaccharide units is manifested in a pseudo-C_2 symmetric spatial structure. The pseudo-C_2 symmetric pyranose backbone of the Le^b tetrasaccharide becomes visible after deleting the ring substituents of Le^b in Figure 5. The four pyranose

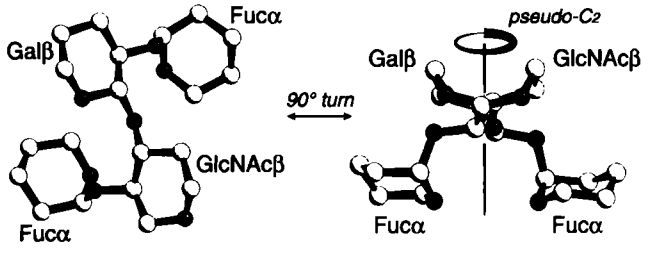

Fig. 5. A pseudo-C_2 symmetric carbohydrate scaffold remains after deleting the ring substituents of the Le^b tetrasaccharide. The pyranose rings are positioned in the corners of a slightly distorted tetrahedron. This secondary structural element fits for all Lewis antigens; the Le^y tetrasaccharide yields an analogous result. The trisaccharides are partial structures of the tetrahedron.

rings are arranged to minimize steric interactions and span a slightly distorted tetrahedron. The two fucoses in the Le^b tetrasaccharide are stabilized by hydrophobic contacts to either *N*-acetylglucosamine or galactose. The ring plane of the fucose connected to 4-O of *N*-acetylglucosamine is about 400 pm distant from galactose; the second fucose is oriented similarly towards *N*-acetylglucosamine (Fig. 4, right). All the Lewis tri- and tetrasaccharides in Figure 4 are superimposable on this structural element, the flexibility of the individual linkages being locked in this globular pseudo-C_2 symmetric motif.

The secondary structural element of Figure 5 is not restricted to the Lewis antigens but holds also for other oligosaccharides as long as the vicinal, bis-equatorial α- and β-connectivity is maintained.

C_2-symmetric Lewis antigen mimetics: The pseudo-C_2 symmetric motif allows the design of totally C_2 symmetric tetrasaccharides. Such substances are readily accessible and form a new class of Lewis antigen mimetics, a topic of current medicinal interest.[7, 21] With only two retrosynthetic steps, the tetrasaccharide f_2g_2 is disconnected to its monosaccharide building blocks (Scheme 2).[22] Not only is synthesis of this β,β-trehalose straightforward, but also structural analysis is simplified by the C_2 symmetry.

Two interglycosidic NOEs define the relative orientation of fucose and galactose: 1b-H–2a-H = 235 pm; 5b-H–2a-H = 270 pm. The β,β-trehalose glycosidic linkage is oriented to minimize steric interactions between the two disaccharide building blocks (Fig. 6a). The resulting tetrahedron is similar to the one spanned by the Le^b tetrasaccharide (Fig. 5), the lengths of sides are between 700 and 900 pm (with 4a-C and 3b-C as corners). Figure 6b shows 10 snapshots of a 100 ps MD run; the relative

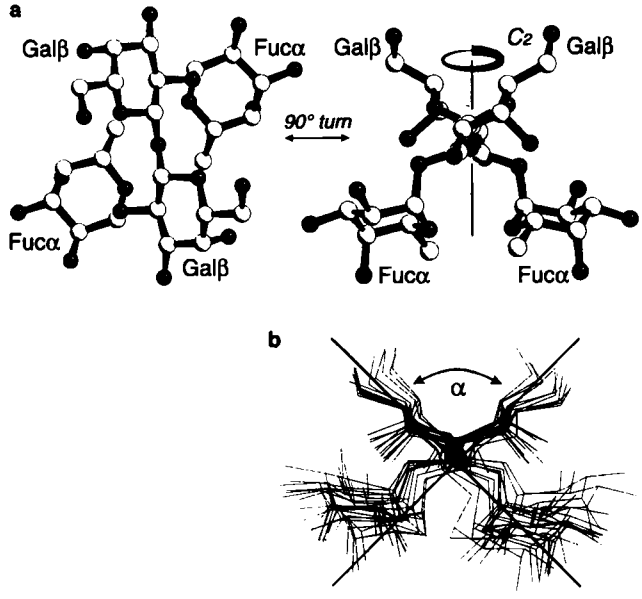

Fig. 6. a) The C_2-symmetric Lewis antigen mimetic f_2g_2. The stacked orientation of galactose and fucose, a characteristic of all Lewis antigens, occurs twice in this compound. Average glycosidic angles for fucose (ϕ = 42°, ψ = 21°) and galactose (ϕ = 50°) are similar to the angles listed in Table 2. b) 10 Snapshots from a 100 ps restrained MD simulation of f_2g_2 at 300 K. The relative mobility of the symmetric disaccharide units is described by α, which varies by less than 30° about an average value of 107°.

mobility of the two Fucα(1 → 2)Galβ units is described by the angle α, which varies between 90 and 120°. Hydrophobic interactions between fucose and the opposite galactose stabilize the globular structure of f_2g_2 and a tightly stacked motif is formed, identical to the one described for the $Lewis^{b/y}$ tetrasaccharide units.

sLe^x with four thioglycosidic bonds: Isosteric substitution of sulfur for oxygen is frequently used to modify conformational features of biopolymers. In spite of the obvious homology of the two elements, the conformational consequences of sulfur within the backbone of carbohydrates are not easy to predict.[23] The C–S bond is about 40 pm longer than the C–O bond and the C^1-S^x-C^x angle smaller (100°) than the C^1-O^x-C^x angle (116°). As a consequence, the distance between two sugars connected by a thioglycosidic bond is increased by 40 pm. A thioglycosidic linkage therefore weakens steric interactions between monosaccharides and allows easier rotation, affecting the adjacent torsion angles ϕ and ψ.[24] Mutual cancellation of dipole moments of the glycosidic oxygens is accompanied by favoured orientations of the glycosidic ϕ angle (*exo*-anomeric effect, electrostatic model[25]). The *exo*-anomeric effect should be weaker for thioglycosides, as was observed for the anomeric effect in thioglycosides.[25, 26] The resulting restriction of glycosidic torsion angles is of little relevance in a polar solvent like water where steric interactions, hydrogen bonding, and the minimization of the solvent-accessible hydrophobic surface (hydrophobic effect) dominate the conforma-

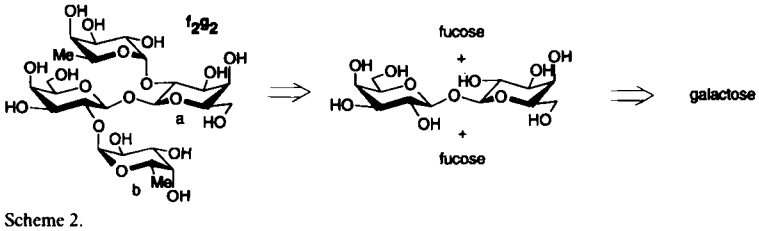

Scheme 2.

tional equilibrium of a carbohydrate.[27] To exclude the possibility of an overestimation of the *exo*-anomeric effect in the computer simulations, we did not include the *exo*-anomeric effect as an additional torsional force either for glycosides or for the thioglycoside. The interpretation of NMR data, as performed for the natural Lewis antigens, was used to describe the conformational behaviour of the sLe^x-mimetic thio-sLe^x[28] in D_2O.

Previous analyses of thioglycosides treated linear carbohydrates and demonstrated the high flexibility of the thioglycosidic bond.[29, 30] The branched trisaccharide unit Galβ(1 → 4)-[Fucα(1 → 3)]GlcNAcβ with thioglycosidic bonds is contained in tetrasaccharide thio-sLe^x and the influence of the increased spacing between the monosaccharide units in thio-sLe^x on the NOE pattern can be compared with the structure of the natural Le^x trisaccharide. Magnetic anisotropy of the C–S bonds led to well-resolved NMR signals, as visible from the expansion of the ROESY spectrum of thio-sLe^x (Fig. 7). Correlations definitely

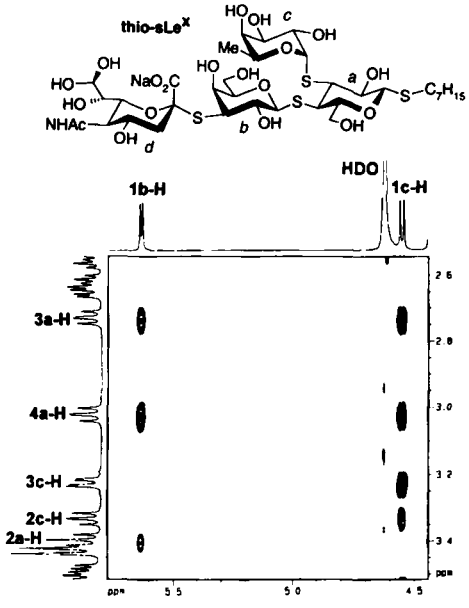

Fig. 7. Expansion of the ROESY spectrum (300 K, 600 MHz) of **2** in D_2O. Two intense ROEs are dectected for each of the anomeric protons of fucose and galactose and the preceding glucose.

absent or very weak in the Le^x series (i.e., a proton–proton distance of >400 pm, Fig. 8) give rise to intense ROEs in thio-sLe^x. The opposite is found for the very reproducible NOE contact between fucose H-5 and galactose H-2, highlighted in Tables 1 and 2; this correlation is absent in thio-sLe^x.

The differences in geometry between oxo- and thiosugars are visible in Figure 8. Fucose and galactose are about 400 pm apart in the oxo-compound (Fig. 8a) and hydrophobic interactions stabilize the stacked *syn/syn* arrangement (*syn* orientation of anomeric proton and transglycosidic proton, $\phi \approx 50°$, $\psi \approx 0°$) of the two pyranose chairs. Figure 8b shows the *syn/syn* conformer of thio-sLe^x with the same glycosidic angles. Fucose and galactose are ca. 500 pm apart at their anomeric carbons and 650 pm at C-4. Thus, not only is the steric interaction with glucose reduced, but the two pyranose rings also lose the hydrophobic contacts with each other. The anomeric proton of fucose shows an intense NOE to glucose 3-H (290 pm), indicating the *syn* conformation found for the oxo-analogous carbohydrate.[31] But there is an additional NOE (270 pm) to glucose 4-H which is only reasonable with an *anti* conformation (*anti* orientation of

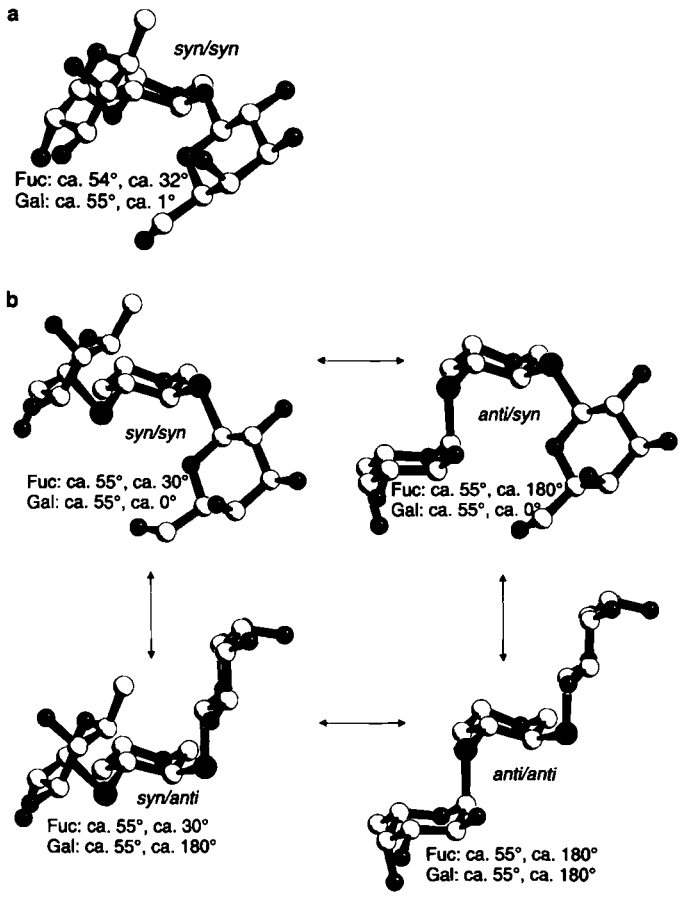

Fig. 8. a) The Le^x trisaccharide of Fig. 4 displayed from a different angle. Fucose (ϕ = 54°, ψ = 32°) and galactose (ϕ = 55°, ψ = 1°) are connected to the vicinal oxygens 3 and 4 of *N*-acetylglucosamine, which is shown without further ring substituents for clarity. b) Four different conformers of the trisaccharide unit of thio-sLe^x (the ring substituents of glucose are again deleted except for fucose and galactose). In the *syn/syn* conformer the distance between fucose and galactose is 100 to 250 pm longer than in sLe^x. The conformational equilibrium of thio-sLe^x is described by the four structures *syn/syn*, *syn/anti*, *anti/syn* and *anti/anti*.

Table 4. Interglycosidic proton–proton distances (pm) of thio-sLe^x.

2	r	2	r
1b-H–2a-H	350	**1c-H–3a-H**	**270**
1b-H–3a-H	290	1c-H–5a-H	310
1b-H–4a-H	**270**	2c-H–4a-H	330
2b-H–3a-H	350	3c-H–3d-H^{ax}	360
2b-H–4a-H	310	**2c-H–5b-H**	**>400**
5b-H–2a-H	**300**	**2c-H–6b-H**	**>400**
1c-H–4a-H	280		

anomeric proton and transglycosidic proton, $\phi \approx 50°$, $\psi \approx 180°$) of the Fucα(1 → 3-S)Glc bond. No combination of glycosidic angles can explain both NOEs simultaneously. The two NOEs are therefore a result of conformational averaging which is too fast to be resolved by NMR spectroscopy.[32] At least two different relative orientations of fucose and glucose must contribute to the solution structure of thio-sLe^x. Galactose exhibits a similar behaviour: two strong NOEs are also found between galactose 1-H and glucose. Besides the NOE indicating *syn* orientation (1b-H–4a-H = 280 pm), there is a NOE for *anti* orientation (1b-H–3a-H = 270 pm). Thus, the thioglycosidic linkages Fucα(1 → 3-S)Glc and Galβ(1 → 4-S)Glc in thio-sLe^x exhibit at least two rotamers each (Fig. 8b).

0947-6539/96/0208-0986 $ 15.00+.25/0 Chem. Eur. J. 1996, 2, No. 8

There are too few NMR data for thio-sLe^x to permit assignment of all participating conformers, and the computational data alone cannot describe a thioglycoside in a realistic manner. Figure 8b shows the accessible conformational space of the thiotrisaccharide moiety Galβ(1 → 4-S)[Fucα(1 → 3-S)]-GlcNAcβ of thio-sLe^x. Fucose and galactose can populate the *syn* ($\phi \approx 50°$, $\psi \approx 0°$) and *anti* ($\phi \approx 50°$, $\psi \approx 180°$) orientation of the glycosidic linkage, respectively. Probably four distinct orientations with *syn/syn*, *syn/anti*, *anti/syn* and *anti/anti* arrangements contribute to the spatial structure of the trisaccharide unit of thio-sLe^x. The absence of long-range NOEs and the detection of additional NOEs between directly connected sugars are typical for flexible compounds and contrast with the NOE pattern observed for the natural oligosaccharides.

Membrane anchoring of the dimeric Lewis glycosphingolipids: Although the branched units of the natural Lewis oligosaccharides are structurally very similar, as pointed out above, the interchanged connectivity at the *N*-acetylglucosamine results in different features for the higher oligomers of the Le$^{x/y}$ and the Le$^{a/b}$ series. sdiLe^x and diLe^y are assembled from alternating (1→3)/(1→4) connected monosaccharides. Both glycolipids and also their higher oligomers form a linear extended chain (Fig. 3, left). Clearly different features are found for diLe^b, the backbone of which is formed by only (1 → 3)-connected carbohydrates (except for lactose). A bent structure with a right angle between tri- and tetrasaccharide units results for diLe^b (Fig. 3, right). Higher oligomers of the Le$^{a/b}$ series (their existence in biological systems is not yet proven) will therefore probably be helical.

The Lewis oligosaccharides are connected to ceramide through the anomeric carbon of glucose, and although NOEs could be detected in this region, it was not possible to interpret the proton–proton distances with a single conformational minimum (e.g., for Le^y: 1a-H–1cer-H$^{low\ field}$ = 260 pm, 1a-H–1cer-H$^{high\ field}$ = 220 pm, 1a-H–2cer-H = 270 pm). Rotation around the bonds connecting lactose and the ceramide aglycon is not fully constrained and NOEs are probably influenced by conformational averaging.

Figure 9 shows a model for the presentation of the Lewis antigens at the membrane surface with a perpendicular orientation of lactose relative to the membrane, an orientation also found for a comparable membrane-anchored carbohydrate.[33] Rotating around their axis, oligomeric Lewis antigens describe a cone, long and slender in the case of diLe^y (Fig. 9, left), short and wide in the case of diLe^b (Fig. 9, right). Thus, the recognition domains of the dimeric Lewis antigens are presented in different ways at the cell surface and the formation of microaggregates[34] will be affected by this.

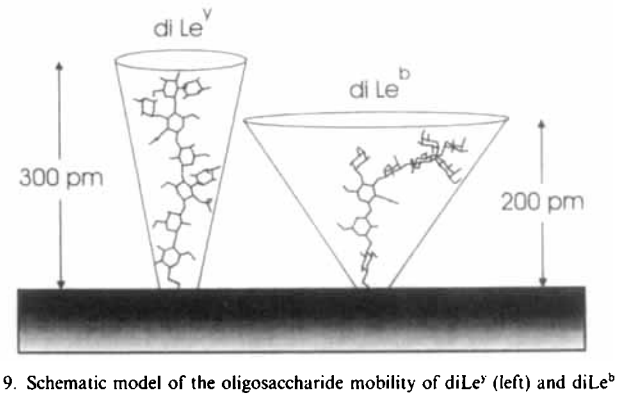

Fig. 9. Schematic model of the oligosaccharide mobility of diLe^y (left) and diLe^b (right) at the membrane surface. Cones are drawn around the glycolipids to underline the differing rotational behaviour. The extended structure of diLe^y reaches further into the periplasmic space than diLe^b.

Conclusion

The spatial structures of the oligomeric Lewis antigens are separable into flexible and rigid domains. The lactose moiety acts as a flexible link between the cell membrane and the first Lewis trisaccharide unit. The GlcNAcβ(1 → 3)Gal linkage connects rigid trisaccharide building blocks with the globular (pseudo-C_2 symmetric) headgroups that are the most restricted motifs of the Lewis glycoconjugates. A real secondary structure dominates the Le^y and Le^b tetrasaccharide building blocks, because orientation of the four pyranose rings depends only upon their connectivity and sugars can be exchanged with minimal structural consequences. This carbohydrate scaffold is well-suited for the design of new, totally C_2-symmetric selectin inhibitors that present two binding domains in one compound.

Experimental Section

All NMR experiments were executed with a Bruker DRX600 spectrometer at a proton resonance frequency of 600.13 MHz. Spectra were recorded at 300 K and chemical shifts were calibrated to internal HDO (δ = 4.67). Homo- and heteronuclear NMR signal assignment was performed in D_2O with the glycolipids connected to a short alkyl spacer (methoxycarbonyloct-1-yl for Le^b and Le^a, azidohexyl for diLe^b, sLe^x, sdiLe^x and diLe^y). TOCSY [35] and DQF-COSY [36] spectra permitted the assignment of the proton spin systems, proton-bearing carbons were identified from HMQC [37] spectra, and sequential assignment of the monosaccharides was obtained from $^2J_{C,H}$ and $^3J_{C,H}$ coupling constants in HMBC [38] spectra. The same procedure was applied to f_2g_2 and thio-sLe^x.

NOESY spectra with a mixing time of 150 ms were recorded for the dimeric Lewis antigens: NMR tubes contained a maximum of 10 mg oligosaccharide connected to the spacers mentioned above. NOEs were interpreted according to the two-spin approximation and calibrated (r^{-6} dependence of the NOE [39]) to one well-resolved intraglycosidic NOE (1-H–3-H = 250 pm in GlcNAc, Gal, or Glc; 4-H–6-H(Me) = 280 pm in fucose for NOEs to methyl groups). Several more intraglycosidic NOEs in each oligosaccharide allowed checking of the calibration. For the two fucose units in sdiLe^x only 5-H and 6-H are well resolved; the homology of the two trisaccharide blocks leads to almost complete signal overlap for protons 1-H to 4-H. The overlapping NOEs to the two anomeric protons of fucose are calibrated from the overlapping intraglycosidic NOEs fucose 1-H–2-H = 240 pm. Overlap of fucose resonance signals in diLe^y and diLe^b was treated in a similar way.

NOESY spectra with a mixing time of 70 or 80 ms were acquired for the monomeric Lewis antigens: NMR tubes contained a maximum of 6 mg oligosaccharide connected to ceramide in 0.5 mL of 320 mmolar solution of [D_{25}]SDS in D_2O. NOEs were interpreted according to the two-spin approximation as described above.

For f_2g_2 and thio-sLe^x, compensated ROESY [40] spectra were acquired (150 ms mixing time, offset correction of peak intensities; again intraglycosidic ROEs served for calibration of interglycosidic ROEs. All 2D experiments were recorded in the phase-sensitive mode by means of time-proportional phase incrementation. Data matrices contained 2048 points in f2 and 512 points in f1. For data processing the matrices were one-time zero-filled in both dimensions followed by apodization with a squared sine bell function shifted by $\pi/2$ in both dimensions. For the HMBC spectra a magnitude calculation was performed in the f2 dimension.

MD simulations which were performed with the force field MM + (*HyperChem* [41]), an extension of MM2 developed by Allinger [42]. Electrostatic contributions were simulated by bond dipole moments associated with polar bonds. Simulations were performed with ethyl aglycons; no explicit solvent molecules and no torsional force to simulate the *exo*-anomeric effect were included. Distance restraints were included with a force constant of 3000 kJ mol^{-1} nm^{-2}. Two intraglycosidic NOEs per sugar residue were included to maintain the chair conformations of the monosaccharides. When the structures remained constant after 50 to 100 ps, the following 100 ps were stored for interpretation. 10 snapshots from this 100 ps trajectory were averaged and then energy-minimized without experimental restraints.

^{1}H and ^{13}C chemical shifts and $^3J_{1-H,2-H}$ coupling constants are available as supplementary material from the correspondence authors.

Acknowledgements: This research was supported by the Deutsche Forschungsgemeinschaft and by the Fonds der Chemischen Industrie. The authors thank Prof. A. Hasegawa for supplying Neu5Acα(2→3)Galβ(1→4)[Fucα(1→3)]GlcβOSE (SE = trimethylsilylethyl).

Received: February 9, 1996 [F297]

[1] a) T. Feizi, *Nature* **1985**, *314*, 53–57; b) S. Hakomori, *Sci. Am.* **1986**, *254*, 32–42.
[2] C.-T. Yuen, K. Bezouska, J. O'Brien, M. Stoll, R. Lemoine, A. Lubineau, M. Kiso, A. Hasegawa, N. J. Bockovich, K. C. Nicolaou, T. Feizi, *J. Biol. Chem.* **1994**, *269*, 1595–1598.
[3] G. Garratty, *Immunol. Invest.* **1995**, *24*, 213–232; b) T. Borén, P. Falk, K. A. Roth, G. Larson, S. Normark, *Science* **1993**, *262*, 1892–1895.
[4] Y. Ichikawa, Y.-C. Lin, D. P. Dumas, G.-J. Shen, E. Garcia-Junceda, M. A. Williams, R. Bayer, C. Ketcham, L. E. Walker, J. C. Paulson, C.-H. Wong, *J. Am. Chem. Soc.* **1992**, *114*, 9283–9298.
[5] A. Toepfer, W. Kinzy, R. R. Schmidt, *Liebigs Ann. Chem.* **1994**, 449–464 and references cited therein.
[6] R. U. Lemieux, K. Bock, L. T. J. Delbaere, S. Koto, V. S. R. Rao, *Can. J. Chem.* **1980**, *58*, 631–653.
[7] a) H. Thogersen, R. U. Lemieux, K. Bock, B. Meyer, *Can. J. Chem.* **1982**, *60*, 44–57; b) R. U. Lemieux, *Chem. Soc. Rev.* **1989**, *18*, 347–374; c) ref. [4]; d) K. E. Miller, C. Mukhopadhyay, P. Cagas, A. Bush, *Biochemistry* **1992**, *31*, 6703–6709; e) R. M. Cooke, R. S. Hale, S. G. Lister, G. Shah, M. P. Weir, *ibid.* **1994**, *33*, 10591–10596; f) K. Scheffler, B. Ernst, A. Katopodis, J. L. Magnani, W. T. Wong, R. Weisemann, T. Peters, *Angew. Chem.* **1995**, *107*, 2034–2037; *Angew. Chem. Int. Ed. Engl.* **1995**, *34*, 1841–1844; g) A. Imberty, E. Mikros, J. Koca, R. Mollicone, R. Oriol, S. Pérez, *Glycoconjugate J.* **1995**, *12*, 331–349.
[8] A. Imberty, E. Mikros, J. Koca, R. Mollicone, R. Oriol, S. Pérez, *Glycoconjugate J.* **1995**, *12*, 331–349.
[9] I. Tvaroska, *Curr. Opin. Struct. Biol.* **1991**, *2*, 661–665.
[10] S. W. Homans, *Biochemistry* **1990**, *29*, 9110–9118.
[11] G. Hummel, R. R. Schmidt, synthesis to be published.
[12] J. Jeener, B. H. Meier, P. Bachmann, R. R. Ernst, *J. Chem. Phys.* **1979**, *71*, 4546–4553; C. Macura, Y. Huang, D. Suter, R. R. Ernst, *J. Magn. Res.* **1981**, *34*, 259–281.
[13] C. Bösch, L. R. Brown, K. Wüthrich, *Biochim. Biophys. Acta* **1980**, *603*, 298–312.
[14] a) D. Kallick, *J. Am. Chem. Soc.* **1993**, *115*, 9317–9318; b) W. Guba, R. Haessner, G. Breipohl, S. Henke, J. Knolle, V. Santagada, H. Kessler, *ibid.* **1994**, *116*, 7532–7540.
[15] D. Acquotti, L. Poppe, J. Dabrowski, C.-W. v. d. Lieth, S. Sonnino, G. Tettamanti, *J. Am. Chem. Soc.* **1990**, *112*, 7772–7778.
[16] Z.-H. Jiang, A. Geyer, R. R. Schmidt, *Angew. Chem.* **1995**, *107*, 2730–2734; *Angew. Chem. Int. Ed. Engl.* **1995**, *34*, 2520–2524.
[17] J. L. Asensio, J. Jimenez-Barbero, *Biopolymers* **1995**, *35*, 55–73.
[18] a) C. Mukhopadhyay, K. E. Miller, C. A. Bush, *Biopolymers* **1994**, *34*, 21–29; b) A. Bernardi, L. Raimondi, *J. Org. Chem.* **1995**, *60*, 3370–3377.
[19] D. F. Mierke, M. Kurz, H. Kessler, *J. Am. Chem. Soc.* **1994**, *116*, 1042–1049.
[20] Ring substituents of *N*-acetylglucosamine have little influence on the orientation of fucose and galactose. Also an exchange of *N*-acetylglucosamine in the sLe^x tetrasaccharide for glucose preserves all relevant NOE contacts (e.g., Fuc-H5–Gal-H2 = 250 pm).
[21] U. Sprengard, G. Kretzschmar, E. Bartnik, C. Hüls, H. Kunz, *Angew. Chem.* **1995**, *107*, 1104–1107; *Angew. Chem. Int. Ed. Engl.* **1995**, *34*, 990–993.
[22] S. Reinhardt, R. R. Schmidt, synthesis to be published.
[23] a) M. Blanc-Muesser, J. Defaye, H. Driguez, *Carbohydr. Res.* **1978**, *67*, 305–328; b) O. Kanie, J. Nakamura, Y. Itoh, M. Kiso, A. Hasegawa, *J. Carbohydr. Chem.* **1987**, *6*, 117–128.
[24] S. Pérez, C. Vergelati, *Acta Crystallogr.* **1984**, *B40*, 294–299.
[25] E. Juaristi, G. Cuevas, *Tetrahedron* **1992**, *48*, 5019–5087.
[26] M. A. Pericàs, A. Riera, J. Guilera, *Tetrahedron* **1986**, *42*, 2717–2724.
[27] M. D. Walkinshaw, *J. Chem. Soc. Perkin. Trans. II* **1987**, 1903–1906.
[28] Synthesis of thio-sLe^x: T. Eisele, A. Toepfer, G. Kretzschmar, R. R. Schmidt, *Tetrahedron Lett.* **1996**, *37*, 1389–1392.
[29] K. Mazeau, I. Tvaroska, *Carbohydr. Res.* **1992**, *225*, 27–41.
[30] K. Bock, J. O. Duus, S. Refn, *Carbohydr. Res.* **1994**, *253*, 51–67.
[31] J. Dabrowski, T. Kozár, H. Grosskurth, N. E. Nifant'ev, *J. Am. Chem. Soc.* **1995**, *117*, 5534–5539.
[32] A. E. Torda, R. M. Brunne, T. Huber, H. Kessler, W. F. van Gunsteren, *J. Biomol. NMR* **1993**, *3*, 55–66.
[33] K. P. Howard, J. H. Prestegard, *J. Am. Chem. Soc.* **1995**, *117*, 5031–5040.
[34] S. Hakomori, *J. Biol. Chem.* **1990**, *265*, 18713–18716.
[35] L. Braunschweiler, R. R. Ernst, *J. Magn. Reson.* **1983**, *53*, 521–528.
[36] U. Piantini, O. W. Sørensen, R. R. Ernst, *J. Am. Chem. Soc.* **1982**, *104*, 6800–6801.
[37] L. Müller, *J. Am. Chem. Soc.* **1979**, *101*, 4481–4484.
[38] M. F. Summers, L. G. Marzilli, A. Bax, *J. Am. Chem. Soc.* **1986**, *108*, 4285–4294.
[39] A. Kumar, G. Wagner, R. R. Ernst, K. Wüthrich, *J. Am. Chem. Soc.* **1981**, *103*, 3654–3658.
[40] a) A. A. Bothner-By, R. L. Stephensen, J. Lee, C. D. Warren, R. W. Jeanloz, *J. Am. Chem. Soc.* **1984**, *106*, 811–813; b) A. Bax, D. G. Davies, *J. Magn. Reson.* **1985**, *63*, 207–213; c) C. Griesinger, R. R. Ernst, *ibid.* **1987**, *75*, 261–271.
[41] *HyperChem* program package, Hypercube, Waterloo, Ontario (Canada), **1994**.
[42] N. L. Allinger, *J. Am. Chem. Soc.* **1977**, *99*, 8127–8134.
[43] After preparation of this manuscript, a crystal structure of the Lewis X trisaccharide was published (F. Yvelin, Y. Zhang, J. Mallet, F. Robert, Y. Jeannin, P. Sinaÿ, *Carbohydr. Lett.* **1996**, *1*, 475–482), with a fucose-5H to galactose-2H distance of 264 pm. Thus the spatial structure of Fig. 4 is not only adopted in isotropic solution but also in the solid state.

0947-6539/96/0208-0988 $ 15.00+.25/0